MULLARD LIMITED
Mullard House
Torrington Place
London, WC1E 7HD

CONTENTS

Transformerless field timebase for 90° 625-line colour	102-109
Ratings of Mullard carbon film resistors	110-112
The basis of a design for a reversible drive with regenerative braking	113-120

VOL. 11 No. 105 MAY 1970

Mullard Technical Communications

VOLUME 11 NUMBER 105

May 1970

Mullard Technical Communications

VOLUME 11 NUMBER 105 May 1970

Contents

Transformerless field timebase for 90° 625-line colour *B. E. Attwood and B. J. Simpson* 102

Ratings of Mullard carbon film resistors 110

The basis of a design for a reversible drive with regenerative braking *J. M. Lavallee and J. Merrett* 113

Mullard Technical Communications records new developments in the application of electronics in science, industry, and the home. It contains information on the properties and performance of discrete and integrated semiconductor devices, electronic valves and tubes, and associated magnetic, electrical, electronoptical, and electromechanical components and assemblies. The practical circuits given are, in general, designed to provide the best working conditions and performance for the devices used. The design principles may be used (so far as device ratings allow) for adaptation to meet particular requirements. Current data should be consulted before any circuit is considered for production. Mullard Limited can normally supply only those devices or assemblies listed in the Company's current catalogues. Availability in large quantities should be confirmed.

All information is published in good faith, but because of the wide variety of situations in which this information may be used, we cannot accept any responsibility for loss or damage resulting from unsatisfactory performance. Publication of this information does not imply any authority or licence for the utilisation of any patented feature.

Six issues are published each year. Circulation (free of charge) is limited to equipment designers, research organisations, laboratories, libraries, educational establishments, and engineering consultants. Requests for addition to the mailing list must be made on the official stationery of the establishment concerned. Technical enquiries should be addressed to the Editor, not to the authors or laboratories.

Abstracts, or references to an article, should mention both the source, *Mullard Technical Communications*, and the authors. Requests for republication or translation should be made to the Editor in writing. All articles in *Mullard Technical Communications* are indexed in *British Technology Index*. Abstracts appear in *Current Papers in Physics, Electrotechnology, and Control.*

'Mullard' is the trade mark of Mullard Limited and is registered in most of the principal countries of the world.

Editor: F. A. Sowan Assistant Editor: E. G. Evans
Central Technical Services,
Mullard Limited, Mullard House, Torrington Place, London, WC1E 7HD
Telephone: 01-580 6633 Telex: 264341

© Mullard Limited, 1970

Made and Printed in England by
WIGHTMAN AND COMPANY LIMITED, 1/3 BRIXTON ROAD, LONDON, S.W.9

Transformerless field timebase for 90° 625-line colour

B. E. ATTWOOD AND B. J. SIMPSON
Mullard Central Application Laboratory

UDC 621.397.132: 621.397.335.1

A scanning circuit having no field output inductor and suitable for scanning 90° colour picture tubes operating at 25kV is described. The circuit operates in the class A mode, but one of the output transistors operates simultaneously as a driver and phase-splitter for the other, thus simplifying the earlier stages of the timebase.

The new type of field oscillator uses a silicon controlled switch. This circuit has all the desirable features of the blocking oscillator circuit used previously, but has greater stability and requires no wound components.

INTRODUCTION

Transistor field timebase circuits usually operate in the class A mode with an output inductor which is relatively bulky and costly. Class B circuits have been fully investigated as an alternative approach, but although they provide a solution which avoids the use of an output inductor, they do not lend themselves to the easiest driving arrangements. In particular, they are not as insensitive to component and transistor spreads as directly coupled class A circuits. Crossover distortion can also be a problem.

Directly-coupled class A circuits of the type shown in Fig. 1 are particularly good in these respects because (a) the clamping action of the switch (field oscillator) is carried through the circuit to the output device, and (b) a simple emitter-follower may be used to voltage-drive the output transistor, thus reducing the influence of current gain spreads.

Since it is desirable to achieve the performance of this type of class A circuit but without a choke, a further circuit has been developed in which a transistor replaces the choke and this is shown in Fig. 2. The advantages of class A operation are retained.

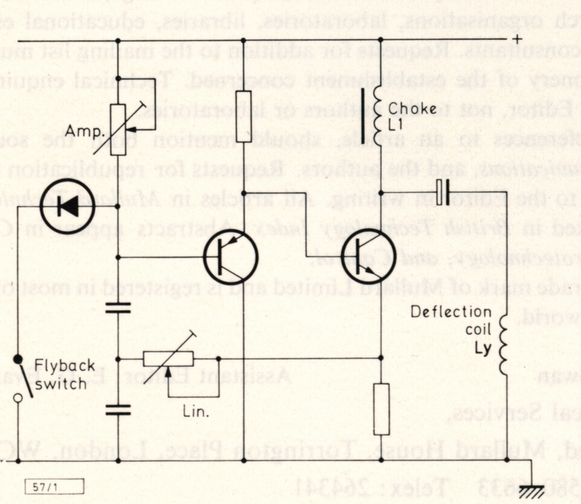

Fig. 1—Directly-coupled class A circuit, with output inductor

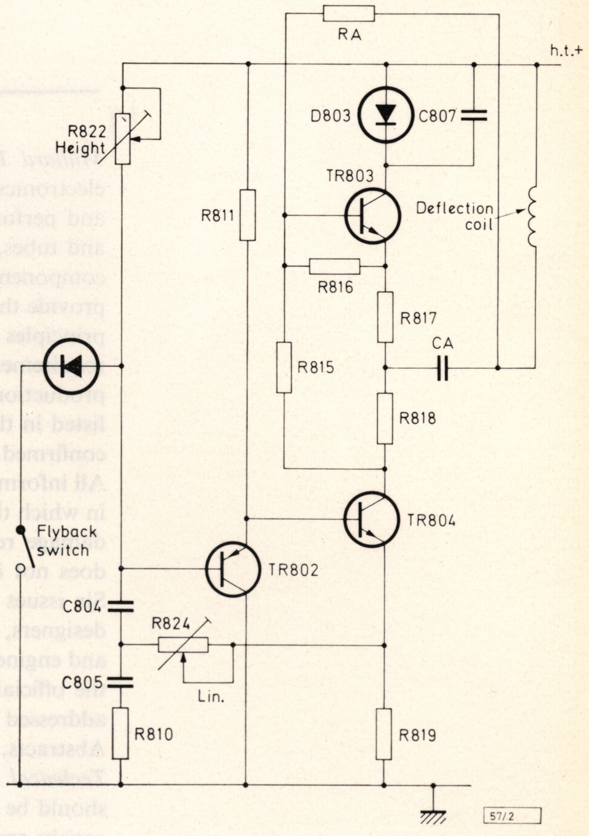

Fig. 2—Basic single-ended push-pull circuit

OUTPUT CIRCUIT

Operation of basic circuit

At the instant that flyback ends and scan begins (that is, as the switch is just opening), TR_{804} is cut off since its base is at chassis potential, TR_{802} being bottomed by the action of the switch. Therefore no current will flow in either TR_{804} or R_{818}. Approximately half the h.t. line voltage V_{ht} will be developed across C_A (that is, the voltage across the deflection coil will swing about V_{ht}, and the voltage at the emitter of TR_{803} will swing about $\frac{1}{2}V_{ht}$). The base-emitter voltage of TR_{803} will, therefore, be dependent primarily on the values of R_{815}, R_A, R_{816}, the input resistance of TR_{803}, and the effective battery voltage across C_A. The value of R_A is chosen to ensure that TR_{803} is conducting when TR_{804} is cut off.

As the scanning stroke progresses, the current in TR_{804} progressively increases, and a voltage develops across R_{818}. At the end of scan, the current through R_{818} is such that the resultant voltage across it cancels the base-emitter voltage present at the base of TR_{803} when TR_{804} was off. Thus, as the scan progresses, the current in TR_{803} decreases while that in TR_{804} increases.

During flyback, TR_{804} is cut off, its base being clamped to chassis potential by the switch and the direct coupling through TR_{802}. As a result of the stored energy in the scanning coils, the voltage across the coils rises positively, and takes the base and emitter of TR_{803} positive. When the rising voltage reaches V_{ht}, diode D_{803} will become non-conductive. The voltage across the deflection coils will then be free to rise to a high value in the form of a half sinewave ring, as shown in Fig. 3, since the deflection coils and C_{807} comprise a resonant circuit. As soon as the voltage is reversed and falls to V_{ht} again, D_{803} will conduct, and a clamping period will occur until the coil current has been fully reversed.

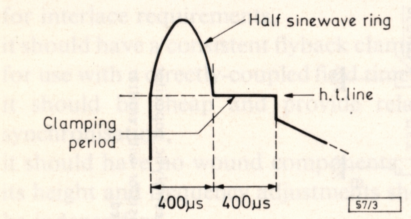

Fig. 3—Collector voltage of TR_{804} during flyback

In effect, it is the energy stored in the scanning coils that must be used for current reversal, but because of the resistive losses in the scanning coils, and external circuitry, it is not quite sufficient. A clamping period where the effective battery voltage across C_A is connected across the deflection coils is necessary to compensate for these losses, and complete the reversal of the scanning current.

Resistors R_{815}, R_A, and R_{816} in Fig. 2 are chosen for correct operation during flyback. They also provide the necessary d.c. bias irrespective of the a.c. waveform present at the emitter of TR_{803}. Feedback for linearity correction can be obtained from R_{819}; the feedback is applied to the junction of C_{804} and C_{805}.

Practical circuit

Some modifications are required to the basic circuit because of the special d.c. shift and convergence requirements.

In Fig. 2, the base current of TR_{803} will flow through the scanning coils, causing an unwanted component of d.c. shift. This effect has been avoided in the complete timebase circuit of Fig. 4 by using a separate bootstrap network, C_{808}, D_{802}, R_{813}, and R_{814}, to provide the necessary base drive to TR_{803}. The principle of operation remains the same.

To obtain a variable d.c. shift, the coil-coupling capacitor C_A in Fig. 2 has been changed from its original position to that shown by C_{703} in Fig. 4. Adjustment of R_{707} will now enable current in the deflection coils to flow in either direction, to provide a smooth d.c. shift of the picture up or down.

If the e.h.t. supply is unstabilised, to maintain the correct picture aspect ratio with mains and beam-current variations the supply to the charge capacitors (C_{804}, C_{805}) is taken from a d.c. voltage obtained by rectifying the pulse voltage appearing across the line transformer.

The driver TR_{802} is an emitter-follower which is bottomed during flyback periods. This configuration gives a low dissipation in the driver transistor, and firmly clamps the base of the output transistor to chassis potential at each cycle. Furthermore, any change in the base-emitter voltage of the driver transistor with temperature opposes that of the output circuit, thus providing stability of the working point with temperature.

The charge capacitors C_{804} and C_{805} must be of a good quality type, having a capacitance which is stable with life and temperature. It is also important that these capacitors have a low series resistance, and their capacitance should be within ±20% of nominal value. Recommended types are:

C_{804} —Mullard C426AR/G50
C_{805} —Mullard C426AR/F25

The operation of the single-ended push-pull circuit during flyback is described in the appendix.

Operating conditions of output circuit

The following measurements apply to nominal **BD131** output transistors:

E.H.T.		25kV
H.T.		40V
Pk-pk deflection coil current (3% overscan)		882mA
Total field timebase current drawn from supply		315mA
	TR_{804}	TR_{803}
Maximum collector-emitter voltage	64V*	30V†
Peak collector current	550mA	480mA
‘Sit-up’ current	20mA‡	20mA
Dissipation	2·9W	3·0W

* during flyback
† end of scan
‡ at start of scan (no current during flyback period)

Setting-up procedure

During receiver manufacture, the height control R_{822} should be set for minimum scan (that is, maximum resistance value) and the rest of the controls should be set to the mid-point of their range. The sequence of setting-up operations is:

1) adjust the frequency control R_{821} until the circuit is synchronised;
2) adjust the linearity control R_{824} for good linearity of scan;
3) adjust the height and d.c. shift controls R_{822} and R_{707} respectively, for correct 3% overscan and picture centring;

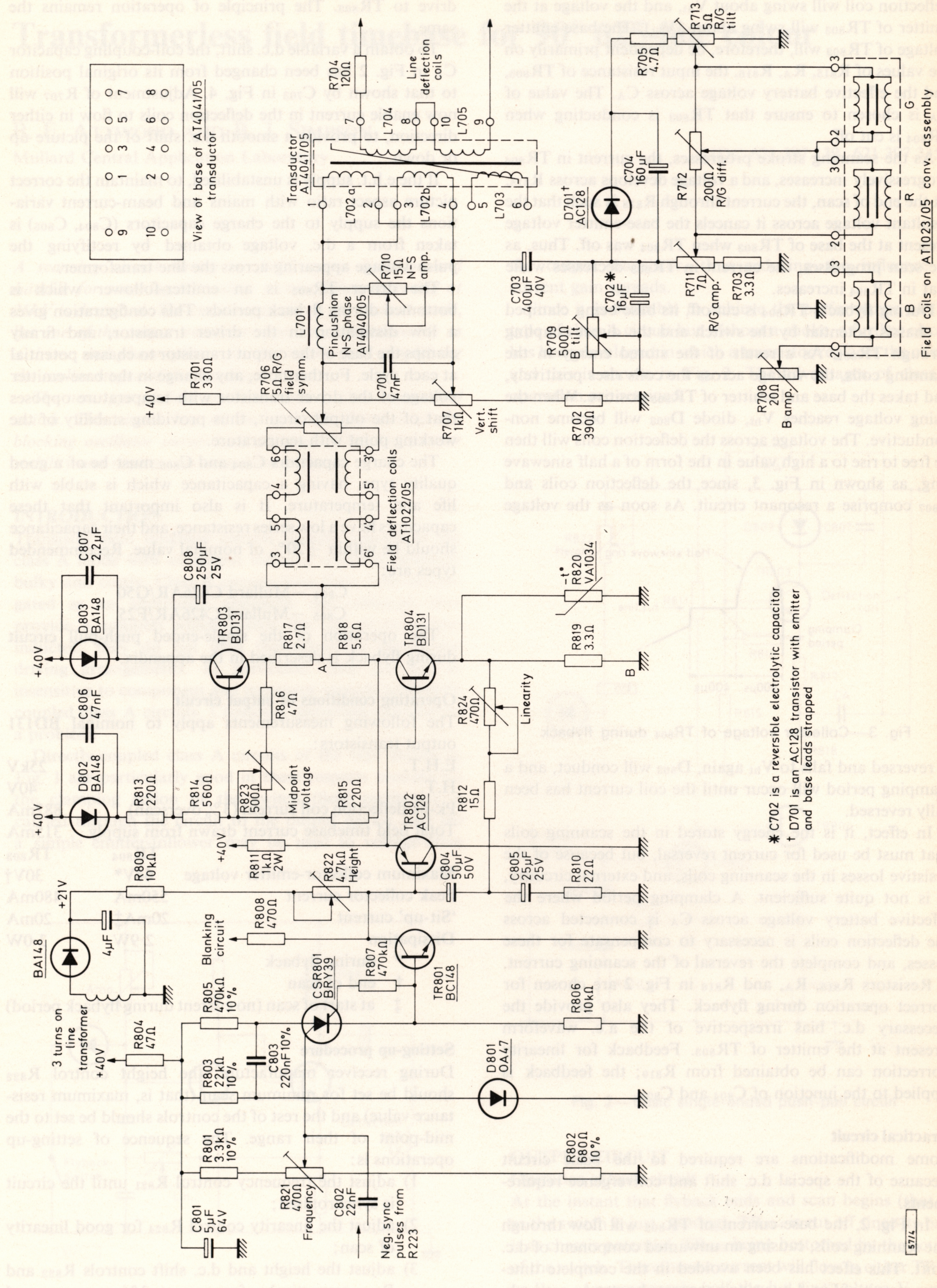
View of base of AT4041/05 transducer
Transducer AT4041/05
Line deflection coils
Pincushion N-S phase AT4040/05
Field deflection coils AT1022/05
Field coils on AT1023/05 conv. assembly
R704 120Ω
R705 4.7Ω
R713 5Ω R/G tilt
D701† AC128
C704 160µF
R712 200Ω R/G diff.
R710 15Ω N-S amp.
C703 400µF 40V
C702* 16µF
R711 7Ω R/G amp.
R703 3.3Ω
R709 500Ω B tilt
R708 20Ω B amp.
R706 5Ω R/G field symm.
R701 330Ω
C701 47µF
R707 1kΩ Vert. shift
R702 390Ω
R820 VA1034
R819 3.3Ω
C807 2.2µF
C808 250µF 25V
D803 BA148
TR803 BD131
R817 2.7Ω
R818 5.6Ω
TR804 BD131
C806 47nF
R816 47Ω
R824 470Ω Linearity
D802 BA148
R813 220Ω
R814 560Ω
R823 500Ω Midpoint voltage
R815 220Ω
TR802 AC128
R812 15Ω
R809 10kΩ
R811 1kΩ 2W
R822 47kΩ Height
C804 25µF 50V
C805 25µF 25V
R810 22Ω
BA148
4µF
3 turns on line transformer
R808 470Ω
Blanking circuit
R807 470kΩ
TR801 BC148
R804 47Ω
R805 470kΩ 10%
CSR801 BRY39
R806 10kΩ
R803 22kΩ 10%
C803 220nF 10%
D801 OA47
R801 3.3kΩ 10%
R821 470Ω Frequency
C802 22nF
C801 5µF 6.4V
R802 680Ω 10%
Neg. sync pulses from R223
+40V
+21V
A
B
57/4

* C702 is a reversible electrolytic capacitor

† D701 is an AC128 transistor with emitter and base leads strapped

Fig. 4—Complete field timebase and convergence circuit

4) adjust the mid-point voltage control R_{823} until the voltage between the transistor end of the scanning coil (point A) and the negative line (point B) is 22±1V;
5) readjust the height and linearity, if necessary;
6) carry out field dynamic convergence.

Deflection coils

The timebase design is based on the Mullard deflection unit type AT1022/05, the field coils being connected in series parallel. Measurements taken on the coil are:

Inductance at 1kHz	24mH
Resistance at 20°C	14Ω
Pk-pk current for edge-to-edge scan at 25kV	855mA
Pk-pk current for 3% overscan at 25kV	882mA

No thermistor is required in series with the coils (in contrast to the valve field timebase circuit published previously, Ref.1)

OSCILLATOR CIRCUIT

Field oscillator requirements

The field oscillator should have the following properties:
1) it should be capable of good triggering stability for interlace requirements,
2) it should have a consistent flyback clamping voltage for use with a directly-coupled field timebase circuit,
3) it should be cheap and provide relatively easy synchronisation,
4) it should have no wound components,
5) its height and frequency adjustments should ideally be independent.

Existing typical field oscillator circuits can be classed as follows: blocking oscillator, multivibrator, self-oscillating multivibrator, and oscillator using a silicon controlled switch.

The blocking oscillator is capable of both good interlace and good stability of operation, but has an inductor which should if possible be avoided.

The multivibrator (and variants of it) has the disadvantage that one of the multivibrator pair is on during the scanning stroke, and can under certain conditions actually amplify both noise on the sync waveform and line pulse pick-up present in the base circuit of the device which is on. This is not conducive to good triggering and often results in poor interlacing. In addition to interlace problems, the operating conditions of the multivibrator tend to be dependent on device spreads.

Simple transistor self-oscillating circuits are not suitable since, when the output transistors are working in a transformerless chokeless circuit, it is essential that the deflection coils be tuned to obtain correct flyback operation. The voltage during flyback will then rise in a half sine-wave. This, coupled with the extensive line frequency filtering required, gives poor switching characteristics of the multivibrator. Interdependence of controls and interlace are also problems.

A circuit using a silicon controlled switch is a new type of oscillator. Like the blocking oscillator it is off during the field scanning stroke, and is, therefore, potentially capable of good interlace. Moreover, it does not require any inductors, and has a very constant clamping voltage.

Silicon controlled switch

A silicon controlled switch (SCS) is a four-layer (three junction) device similar to a thyristor, but all four layers are accessible as terminals. Fig. 5a shows the sequence of the layers, the type of material, and the usual names given to the terminals. Fig. 5b shows the similarity between a pair of complementary transistors and the SCS, which is useful in understanding the electrical characteristics of the SCS. Fig. 5c shows the symbol used in this article.

When the anode is made positive with respect to the cathode, and the gates are open-circuit, a very small leakage current will flow in the anode. If the anode voltage is increased until the breakdown region is reached, the anode current will increase until the current gain of the internal transistor action reaches a value of unity, as shown in Fig. 6a. At this point another effect is taking place as shown in Fig. 6b; the anode-cathode path slope resistance

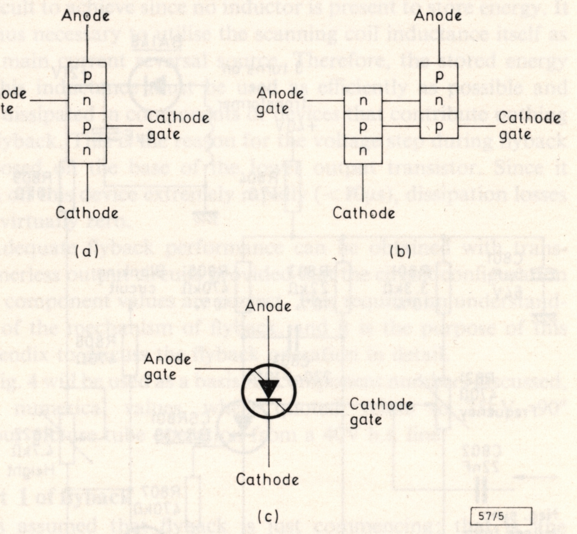
Anode
Anode gate
Cathode gate
Cathode
p
n
p
n
(a)
(b)
(c)
57/5

Fig. 5—Silicon controlled switch
a) four-layer structure
b) equivalent in terms of transistors
c) symbol

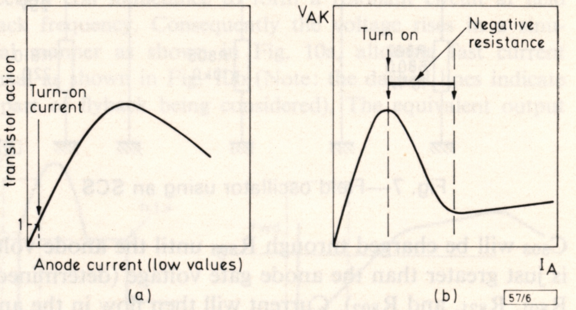

Fig. 6—Characteristics of SCS during turn-on
a) current gain of internal transistor action plotted against anode current
b) anode-cathode voltage plotted against anode current.

is changing from positive to negative. When this point is passed, the SCS turns on, thus assuming a low impedance.

The SCS will remain on provided that a current above a critical value known as the turn-off or holding current continues to flow. When the anode current falls below the holding value, there is insufficient internal gain and the device returns to a high-impedance state.

The device can also be made to turn on at any voltage below its breakdown voltage by causing either of the gates to be sufficiently forward biased, thus bringing the anode current to the critical value by conventional transistor action.

Field oscillator circuit description

The circuit diagram of a field oscillator for use with transistor field timebases is shown in Fig. 7.

If the capacitor C_{803} is fully discharged and the SCS, CSR_{801}, is in the off (high-impedance) condition, diode D_{801} will then be forward-biased by the current through R_{803}. Therefore, the junction of D_{801} and C_{803} will be substantially clamped to the zero-volt line. Capacitor C_{803} will be charged through R_{805} until the anode voltage is just greater than the anode gate voltage (determined by R_{801}, R_{821}, and R_{802}). Current will then flow in the anode gate causing CSR_{801} to assume a low-impedance on-state. The current through CSR_{801} resulting from both the discharge current of capacitor C_{803} and the current through R_{801}, will flow through the base-emitter junction of TR_{801}, turning the transistor on.

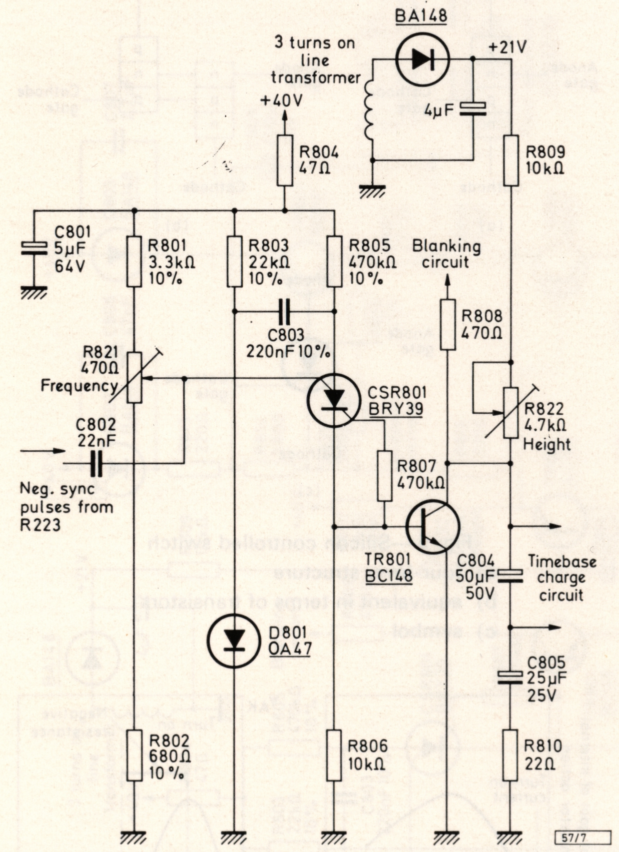

Fig. 7—Field oscillator using an SCS

Unlike earlier circuits, which employed a simple discharge resistance in series with C_{803}, and gave an exponential decay of current, the combination of R_{803} and D_{801} causes an almost constant discharge to flow through C_{803}, CSR_{801} and the base-emitter of TR_{801} during the flyback period. When the capacitor has fully discharged, and the voltage across the capacitor is about to reverse (aiming towards h.t. supply voltage through R_{803}), diode D_{801} will very abruptly conduct. As a consequence, the constant current flowing through R_{803}, C_{803}, and CSR_{801} will be diverted to a new path R_{803} and D_{801}. Since the current through CSR_{801} has been abruptly reduced to a value less than the holding current, the device turns off.

It can be seen, therefore, that the flyback time is dependent on the values of R_{803} and C_{803}, and the scanning period upon the values of R_{805} and C_{803}. Both times are also dependent on the setting of R_{821} (under the free-running condition only).

In the directly-coupled field timebase, the 'sit-up' current in the output stage is dependent on the oscillator flyback period. This is because the charge (and thus the degree of 'sit-up') remaining on the charge capacitors at the end of flyback is dependent on the time of discharge. Since the 'sit-up' current is required to remain within certain limits, it follows that the oscillator flyback time, which is dependent on component and active device spreads, and temperature variations, must also remain within certain limits.

Components R_{803} and D_{801} are particularly effective in stabilising the flyback time for a given setting of R_{821}. The setting of R_{821} to give a 20ms overall period is only dependent on the tolerances of R_{805} and C_{803}. Therefore, the flyback time is quite closely controlled for a given frequency of operation.

The circuit has been arranged so that, when the frequency control R_{821} is varied (applicable for the unsynchronised condition only), the flyback time and 'sit-up' current vary in such a way that the variation in total timebase supply current is reduced. This is because the 'sit-up' current becomes smaller at lower oscillator frequencies, whereas it is usual for the total circuit current to rise at lower frequencies, giving rise to high output device dissipations in out-of-sync conditions. This mode of operation, therefore, gives safer operating conditions, and allows the use of smaller heatsinks for the output devices than is normally possible.

However, the flyback time and 'sit-up' current do remain constant whenever the circuit is synchronised, irrespective of the setting of R_{821}, since the charge on C_{802} will remain constant for the correct scanning time, and this time is set by the sync pulses.

For the purposes of synchronisation, CSR_{801} may be triggered by negative pulses in the anode gate or positive pulses in the cathode gate. R_{807} forms a d.c. path for the positive sync pulses and cathode gate leakage currents. R_{806} prevents TR_{801} being turned on by leakage currents during the scanning period.

No sync pulse amplifier is required when CSR_{801} is triggered by the anode gate. Thus a considerable price advantage is obtained over existing circuits. The circuit in Fig. 8 gives good interlace and generally good sync performance.

The cathode gate, however, requires a relatively 'clean' signal. If a very 'noisy' signal is used, it has the disadvantage that large interference pulses can turn TR_{801} on directly, thus upsetting the charging of the charge capacitors C_{804} and C_{805}. A method which does allow relatively poor positive sync pulses to be used is shown in Fig. 9.

When CSR_{801} is on, approximately 12mA flows through R_{801}, into the anode gate and out of the cathode, into the base of TR_{801}. The current increases the turn-off current of the device, which makes the circuit more tolerant of certain SCS spreads, and further stabilises the flyback time. During scanning, TR_{801} is off and the charge capacitors C_{804}, C_{805} charge up. When CSR_{801} triggers, TR_{801} is turned hard on, and the capacitors are discharged. One advantage of this circuit is the low and consistent voltage drop across TR_{801} at the end of flyback, which ensures a very constant working point for the output transistors. Furthermore, independence of amplitude and frequency adjustment is obtained.

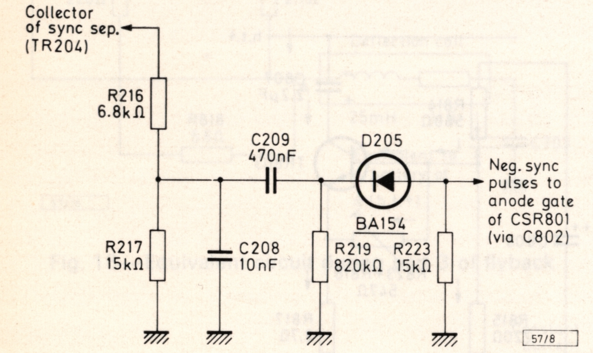
Collector of sync sep. (TR204)
R216 6.8kΩ
C209 470nF
D205
BA154
Neg. sync pulses to anode gate of CSR801 (via C802)
R217 15kΩ
C208 10nF
R219 820kΩ
R223 15kΩ
57/8

Fig. 8—Field sync circuit for use with negative sync pulses

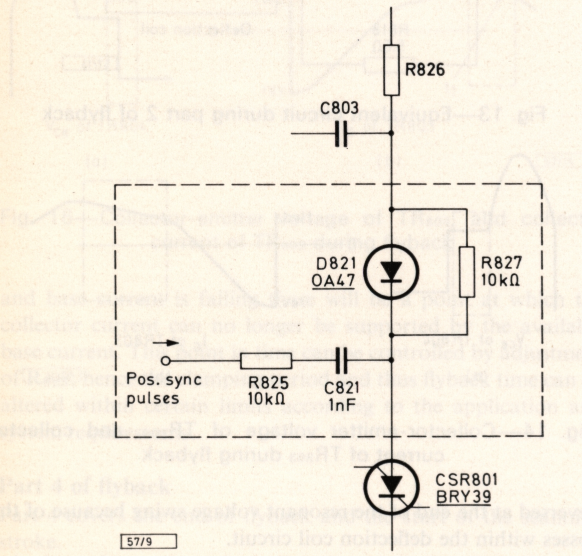

Fig. 9—Field sync circuit for use with positive sync pulses

The circuit using negative sync pulses, shown in Figs. 4 and 7, was tested over the temperature range —20 to + 85°C. There was found to be less than 2% change in the frequency (free running condition) and less than 2% change in flyback time.

REFERENCES

1. BOULTON, P. G., 'Field timebase', **Mullard Technical Communications**, Vol. 9, No. 83, September 1966, pp. 67 to 69.

APPENDIX

Operation of the single-ended push-pull circuit during flyback

In field timebase circuits employing transformer or choke output configurations, complete reversal of the deflection coil current is easily obtained because of the extra stored energy available in the choke or transformer.

In transformerless chokeless circuits, however, flyback is more difficult to achieve since no inductor is present to store energy. It is thus necessary to utilise the scanning coil inductance itself as the main current reversal source. Therefore, the stored energy in this inductance must be used as efficiently as possible and not dissipated in components or devices that contribute nothing to flyback. This is the reason for the voltage step during flyback imposed on the base of the lower output transistor. Since it cuts off this device extremely rapidly (<10µs), dissipation losses are virtually zero.

Adequate flyback performance can be obtained with transformerless output circuits provided that the circuit configuration and component values are correct. This requires an understanding of the mechanism of flyback, and it is the purpose of this appendix to discuss the flyback operation in detail.

Fig. 4 will be used as a basis for component numbers discussed, and numerical values, where quoted, relate to 25kV, 90° colour picture tube operation from a 40V h.t. line.

Part 1 of flyback

It is assumed that flyback is just commencing; that is, the switch CSR_{801} is closed and the output transistor TR_{804} is just cutting off. The sequence will then be as follows.

At first, the voltage at point A will go positive very quickly because of the stored energy in the deflection coil inductance. When point A goes substantially above the h.t. line, diodes D_{802} and D_{803} become nonconductive, and C_{807} tunes with the deflection coil inductance to form a resonant circuit at field flyback frequency. Consequently the voltage rises in a sinusoidal manner as shown in Fig. 10a, allowing fast current reversal as shown in Fig. 10b (Note: the dashed lines indicate the part of flyback being considered). The equivalent output

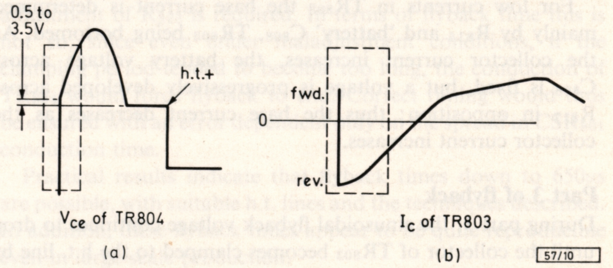

Fig. 10—Collector-emitter voltage of TR_{804}, and collector current of TR_{803} during flyback

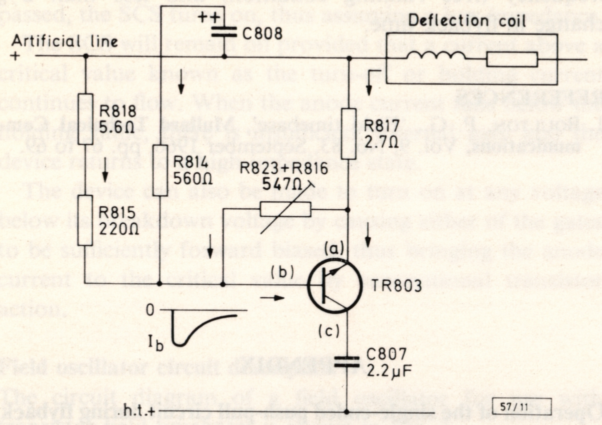

Fig. 11—Equivalent circuit during part 1 of flyback

circuit becomes as shown in Fig. 11, where C$_{808}$, being large, is effectively a battery.

Transistor TR$_{803}$ is now operating in a reverse conduction mode. The necessary base current is predominantly supplied by R$_{814}$, although R$_{815}$ and R$_{818}$ do have some influence because of the voltage drop across R$_{817}$. Ideally, this current should be sufficient to ensure that the transistor TR$_{803}$ is bottomed under the maximum reverse current condition occurring at the start of the flyback stroke. To ensure that this is so would require unnecessarily stringent base network values, or a guaranteed high reverse-mode current gain in TR$_{803}$. If it is assumed, therefore, that the base current is insufficient to support the 'new collector' current (terminal (a) in Fig. 11), the collector-emitter voltage will rapidly increase. Thus, more current will flow via R$_{814}$, R$_{818}$, R$_{815}$ and additionally via R$_{823}$ until the collector current can be supported. The circuit thus stabilises itself against wide spreads of reverse h_{FE}.

A reverse collector-emitter voltage of 3·5V during this instant of flyback will cater for transistors with reverse current gains down to 5. The effect of this voltage on TR$_{803}$ dissipation is negligible, only amounting to additional dissipation in the milliwatt region.

Alternatively, a diode may be used in shunt with TR$_{803}$ to allow the reverse current to flow. However, the device used for TR$_{803}$ has been made suitable for this mode of operation, and so the cost of a high-current shunt diode is saved.

Part 2 of flyback

Part 2 starts as the sinusoidal coil voltage reverses and its current passes through zero. Transistor TR$_{803}$ works in a conventional manner from this instant and for the remainder of the flyback and scanning cycle. The collector-emitter voltage of TR$_{804}$, and the collector current of TR$_{803}$ are shown in Fig. 12. The equivalent circuit is shown in Fig. 13.

For low currents in TR$_{803}$ the base current is determined mainly by R$_{814}$ and 'battery' C$_{808}$, TR$_{803}$ being bottomed. As the collector current increases, the battery voltage across C$_{808}$ is fixed, but a voltage is progressively developed across R$_{817}$ in opposition; thus the base current decreases as the collector current increases.

Part 3 of flyback

During part 3, the sinusoidal flyback voltage continues to drop until the collector of TR$_{803}$ becomes clamped to the h.t. line by conduction of D$_{803}$. A clamping period then occurs, as shown in Fig. 14a. The clamping period is necessary, since, as can be seen from Fig. 14b, the deflection coil current has not fully reversed at the end of the resonant voltage swing because of the losses within the deflection coil circuit.

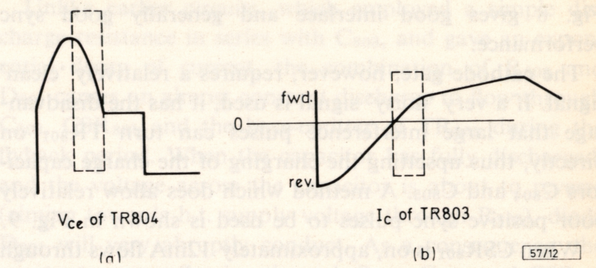

Fig. 12—Collector-emitter voltage of TR$_{804}$, and collector current of TR$_{803}$ during flyback

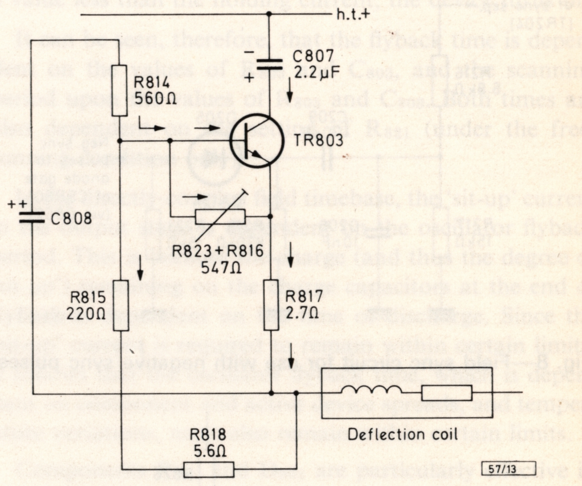

Fig. 13—Equivalent circuit during part 2 of flyback

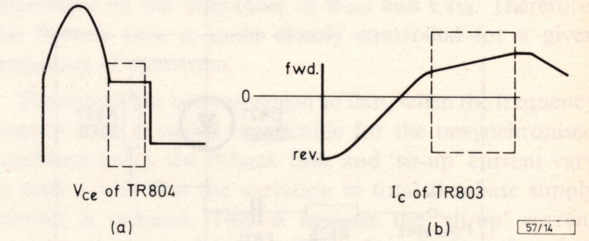

Fig. 14—Collector-emitter voltage of TR$_{804}$, and collector current of TR$_{803}$ during flyback

In Fig. 15 it is shown that the prime cause of continuing reversal of the deflection coil current is the h.t. line voltage minus the effective battery voltage across C$_{703}$. This resultant voltage is clamped across the coils until the current has fully reversed. Voltage drops across D$_{803}$, TR$_{803}$, and R$_{817}$ are small and have been neglected. The circuit in Fig. 4 has a clamping voltage of approximately 18V across the 14Ω deflection coils during this period. Thus the aiming current will be 18/14A, which approximately equals 1·3A, over a period dependent on the LR time-constant of the deflection circuit.

It has already been mentioned in part 2 of the flyback that, as the collector current in TR$_{803}$ increases, the base current is reduced, because the increasing voltage across R$_{817}$ causes the available current from C$_{808}$ and R$_{814}$ to divide between the base path and R$_{815}$. The base path also has a shunt resistance R$_{813}$ plus R$_{816}$ between base and emitter, so the effective base current can be reduced at will, by reducing the value of R$_{823}$.

It follows, therefore, that as the collector current is increasing and base current is falling there will be a point at which the collector current can no longer be supported by the available base current. This point in time can be controlled by adjustment of R$_{823}$; hence the clamping period and thus flyback time can be altered within certain limits according to the application and system requirements.

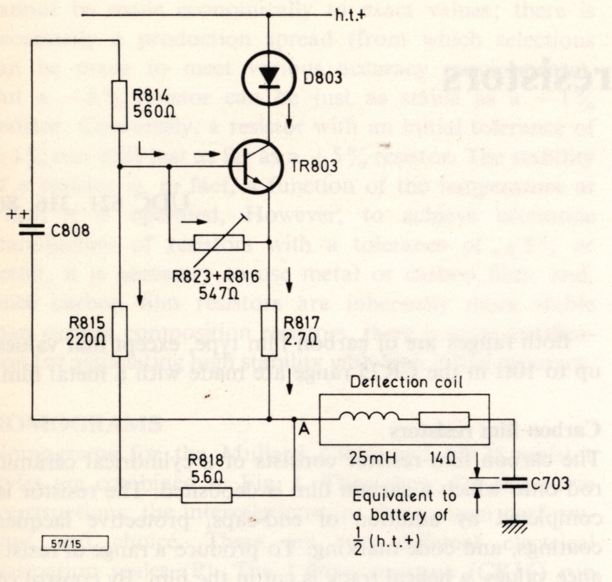

Fig. 15—Equivalent circuit during part 3 of flyback

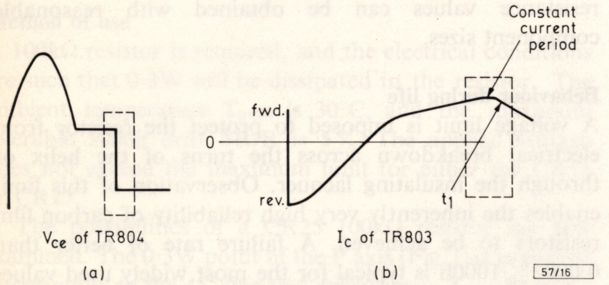

Fig. 16—Collector-emitter voltage of TR$_{804}$, and collector current of TR$_{803}$ during flyback

Part 4 of flyback

Part 4 covers the end of flyback and the start of the scanning stroke.

Part 3 has established that as the collector current of TR$_{803}$ increases, its base current falls, and a time comes when the base current can no longer support the collector current. No more base current can be supplied since C$_{808}$ is a battery source and all resistors are fixed.

As a result, TR$_{803}$ starts to come out of bottoming and rapidly becomes a constant current generator (that is, I_b remains constant irrespective of V_{ce}, since the base drive network is an effective battery network between emitter and base). Therefore, during the clamping period the voltage clamped across the coils is

$$V_{ht}-V_{ce(TR803)}-V_{D803}-V_{R817}-V_{C703}\simeq 18V.$$

When the base current no longer supports the collector current at the predetermined level of say 0·45A, the effective voltage generator across the coils suddenly becomes a constant current generator of 0·45A. The voltage across the coils will, therefore, immediately drop to that value determined by the resistance of the coils and the relevant current; that is,

$$14\Omega\times 0{\cdot}45A=6{\cdot}3V.$$

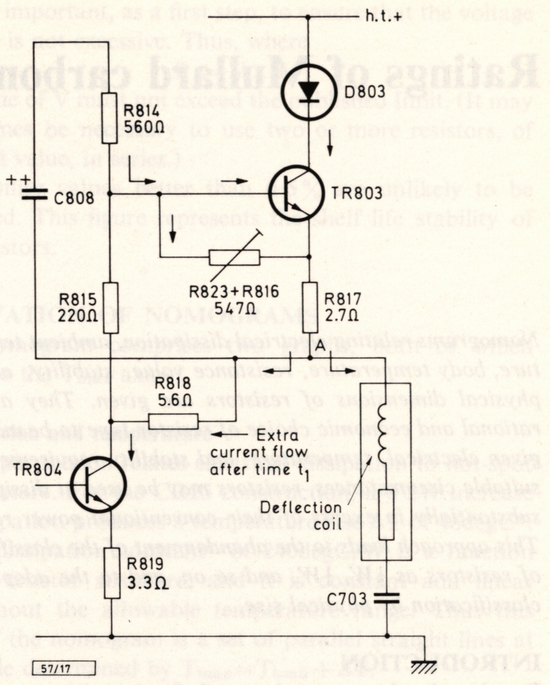

Fig. 17—Equivalent circuit during part 4 of flyback

The inductive component voltage drop across the coils immediately becomes zero. This explains the voltage step in the flyback waveform shown in Fig. 16a, and also why no ringing occurs, since the magnetic flux remains unaltered during this transitional step period. In the example quoted this step voltage will be approximately

$$18-6{\cdot}3V=11{\cdot}7V.$$

The waveforms are shown in Fig. 16, and the equivalent circuit in Fig. 17. The base network of TR$_{803}$ is supplied by the 'battery' C$_{808}$, which controls the constant-current generator TR$_{803}$. Therefore the deflection coil current will be maintained constant (at say 0·45A) until such time as either TR$_{804}$ starts to conduct, altering the bias levels on TR$_{803}$ or, in the limit, if TR$_{804}$ is non-conductive, the time-constant of the effective C$_{808}$ battery network is approached.

In general the conduction of TR$_{804}$ (which is controlled by the pulse duration of CSR$_{801}$) is made to begin equal to, or even slightly longer than, the period needed to fully reverse the scanning coil current.

From the foregoing it might be thought that the flyback time would be very dependent on the h_{FE} of TR$_{803}$, and that critical adjustment of R$_{823}$ is required. In terms of flyback time this is not so, since even under maladjustment conditions, if the clamping period tended to become too long, the conduction of TR$_{804}$ would force flyback to end. Correct timing would thus be ensured with an error dependent only on the spread in CSR$_{801}$ conduction time.

Practical results indicate that flyback times down to 650μs are possible, with suitable h.t. lines and the techniques described. In addition, these flyback times appear to be quite reproducible even in large-scale production.

Ratings of Mullard carbon film resistors

UDC 621. 316. 86

Nomograms relating electrical dissipation, ambient temperature, body temperature, resistance value, stability, and the physical dimensions of resistors are given. They allow a rational and economic choice of resistor type to be made for given electrical, temperature, and stability requirements. In suitable circumstances, resistors may be used at dissipations substantially in excess of their conventional power ratings. This approach leads to the abandonment of the classification of resistors as $\frac{1}{8}$W, $\frac{1}{4}$W, and so on, and to the adoption of classification by physical size.

INTRODUCTION

Despite the large numbers of fixed resistors used in conventional circuits, there is insufficient appreciation of the factors that should determine the choice of a resistor type for a particular set of conditions, or of the interrelationships of these factors. It is, for example, usual to regard the power rating of a resistor as an absolute limit, irrespective of the ambient temperature and the required stability. In this way, unnecessarily large resistors (in terms of power rating and physical dimensions) may be specified, and the equipment may be significantly larger and more expensive than it would have been if a more rational method of choice had been followed.

The ultimate determining factor in the choice of a resistor type is not its power rating but the maximum temperature attained during operation; that is, the "hot-spot" temperature, which normally occurs half-way between the ends of the resistor. The hot-spot temperature is a function of the electrical dissipation and of the ambient temperature; and it is a main determinant of the stability of the resistance value during life.

With data relating to resistors of various physical sizes, the circuit designer is able to specify resistors on the basis of the actual electrical dissipation and the stability that will be achieved. Within the appropriate temperature and voltage limits, stability and electrical dissipation can be traded one for the other; or, as the dissipation and stability are likely to be fixed requirements, the best physical size that will meet both requirements can be chosen. The maximum voltage rating of the resistor must be satisfied; but the supposedly mandatory wattage rating can be ignored. Further, high stability may be obtained with resistors from normal ranges.

RESISTOR STRUCTURE AND BEHAVIOUR

The nomograms (Fig. 1) relate to the Mullard resistor styles CR16 and CR25. The CR16 resistors have a body diameter of 1·6mm; and the CR25, of 2·5mm. These ranges will no longer be known as $\frac{1}{10}$W and $\frac{1}{8}$W resistors.

Both ranges are of carbon film type, except that values up to 10Ω in the CR25 range are made with a metal film.

Carbon film resistors

The carbon film resistor consists of a cylindrical ceramic rod onto which a carbon film is deposited. The resistor is completed by addition of end-caps, protective lacquer coatings, and code-marking. To produce a range of resistance values, a helical track is cut in the film. By control of the film thickness and the effective length and width of carbon track between the terminals, a large range of resistance values can be obtained with reasonable component sizes.

Behaviour during life

A voltage limit is imposed to protect the resistor from electrical breakdown across the turns of the helix or through the insulating lacquer. Observation of this limit enables the inherently very high reliability of carbon film resistors to be achieved. A failure rate of better than 0·0002%/1000h is typical for the most widely used values of resistor.

Disregard of the hot-spot temperature limit can lead to catastrophic failure caused by the protective lacquer lifting from the ceramic rod and pulling away sections of the carbon film. It will, also, certainly reduce the stability of the resistance value.

Life tests have shown that, for conditions within the specified voltage and temperature limits, significant changes in resistance will be substantially complete well within the first 1000 hours. Later changes will be relatively slight. It is therefore reasonable to quote the maximum expected drift of resistance value as $(\Delta R/R)$%/1000h with a probability of 95%.

Accuracy and stability

When a fixed resistor is to be specified, its voltage and current conditions will be known. Thus a resistor with a particular resistance value will be required. The nature of the application will determine the limits that must be placed on this initial value, and on the drift that will be tolerable during life. A resistor with, say, ±5% tolerance on its nominal initial value will be specified. The next step is to choose a resistor that will remain within some required percentage of its initial value. Thus, a resistor with an initial value of 100kΩ±5% may be required to remain within, say, ±2% of its initial value, irrespective of whether that value was 95kΩ or 105kΩ.

The initial accuracy of the resistance value, and the stability during life, are separate questions. Resistors cannot be made economically to exact values; there is necessarily a production spread (from which selections can be made to meet various accuracy requirements). But a −5% resistor can be just as stable as a −1% resistor. Conversely, a resistor with an initial tolerance of ±1% can drift just as far as a ±5% resistor. The stability of a resistor is, in fact, a function of the temperature at which it is operated, However, to achieve economic manufacture of resistors with a tolerance of ±5% or better, it is necessary to use metal or carbon film; and, since carbon film resistors are inherently more stable than carbon composition resistors, there is some justification for associating high stability with high initial accuracy.

NOMOGRAMS

Nomograms for the Mullard CR16 and CR25 resistor styles are combined in Fig. 1. They show, for these two constructions, the interrelationships that govern performance and choice. There are two different electrical dissipation scales (P). The 1·6mm resistors (CR16) run hotter, for a particular dissipation, than the 2·5mm resistors (CR25).

Method of use

A 100kΩ resistor is required, and the electrical conditions are such that 0·3W will be dissipated in the resistor. The ambient temperature T_{amb} is 30°C, and the maximum tolerable 1000h drift $\Delta R/R$ is 5%. The applied voltage does not exceed the maximum limit for either the CR16 or CR25.

The possibilities of a CR25 100kΩ resistor are first examined. The 0·3W point of the P axis (Fig. 1) is projected horizontally to the 45° line that represents a T_{amb} of 30°C. At this ambient temperature the hot-spot temperature (T_{max}) will be T_{amb} plus the temperature rise ΔT produced by the 0·3W dissipation; and it is read off by projecting down to the T_{max} scale. In our example, T_{max} will be 103°C.

If this point is projected down to the sloped line representing a resistance of 100kΩ, and then horizontally to the $\Delta R/R$ scale, the 1000h drift (with 95% probability) is seen to be about 0·6%max.

It may be that 0·6% stability is better than the application demands; or that a physically smaller resistor is desirable. Then, from Fig. 1, it is found that P (CR16) = 0·3W and T_{amb} = 30°C will produce a hot-spot temperature T_{max} = 150°C; and a CR16 100kΩ resistor operating at this temperature will drift about 3·0% max in the first 1000 hours. If this is acceptable, then the CR16 resistor can be used rather than the CR25.

The saving in space will be even greater than that given by using CR16 instead of CR25. For a 0·3W dissipation, the conventional choice would have been not a CR16 ("$\frac{1}{10}$W") or a CR25 ("$\frac{1}{8}$W") but a 0·5W resistor. This component would be considerably larger and (being run very much within its potentialities) quite excessively stable for the application.

Limitations

The maximum hot-spot temperature for both CR16 and CR25 is 155°C. This limit is applied automatically by the nomograms, since the temperature scales are cut off at this temperature.

It is important, as a first step, to ensure that the voltage present is not excessive. Thus, where

$$P = V \times I$$

the value of V must not exceed the published limit. (It may sometimes be necessary to use two or more resistors, of reduced value, in series.)

Stability values better than 0·5% are unlikely to be obtained. This figure represents the shelf life stability of the resistors.

DERIVATION OF NOMOGRAMS

The nomogram comprises two graphs, both of which relate to the T_{max} axis.

Dissipation and temperature

The upper section relates electrical dissipation to hot-spot temperature. For the CR25 construction, a 0·2W increase in dissipation produces a temperature rise ΔT of 48degC*. This "dissipation constant" of 240degC/W is a function of the resistor structure, and it is constant and linear throughout the allowable temperature range. Thus this part of the nomogram is a set of parallel straight lines at an angle determined by $T_{max} = T_{amb} + \Delta T$.

The limit T_{max} = 155°C means that, in the extreme case of T_{amb} = 155°C, the allowable temperature rise ΔT (and therefore the dissipation P) must be nil.

Temperature and stability

The lower part of the nomogram shows the exponential relationship of hot-spot temperature T_{max} and 1000h resistance drift $\Delta R/R$ for various values of resistor. It is based on statistical analysis of the results of extensive life tests. The $\Delta R/R$ values are the greatest drifts (with a probability of 95%) that will be experienced. The majority of resistors from a batch will drift less than the $\Delta R/R$ scale indicates.

Resistance drift, in resistors of any particular value and construction, is a function of hot-spot temperature, no matter how this temperature is attained. Thus a 1MΩ resistor from the CR25 range, operating at a hot-spot temperature T_{max} = 120°C, will show a maximum drift of about 2% under any of the following conditions:

T_{amb} (°C)	P (W)
20	0·41
60	0·25
100	0·08
120	0

These sample operating conditions, it is worth noting, are for a resistor that was conventionally rated at P = 0·125W.

Resistance drift $\Delta R/R$ at a given temperature is determined, mainly, by the thickness of the carbon film. For a given body size, the lower value resistors give a better stability than the higher values. Thus, a 10MΩ resistor from the CR25 range, operating at (say) a hot-spot temperature of 90°C, has a probable maximum drift of

---

* The comparable increase for the physically smaller CR16 construction is about 80 degC, or 400 degC/W.

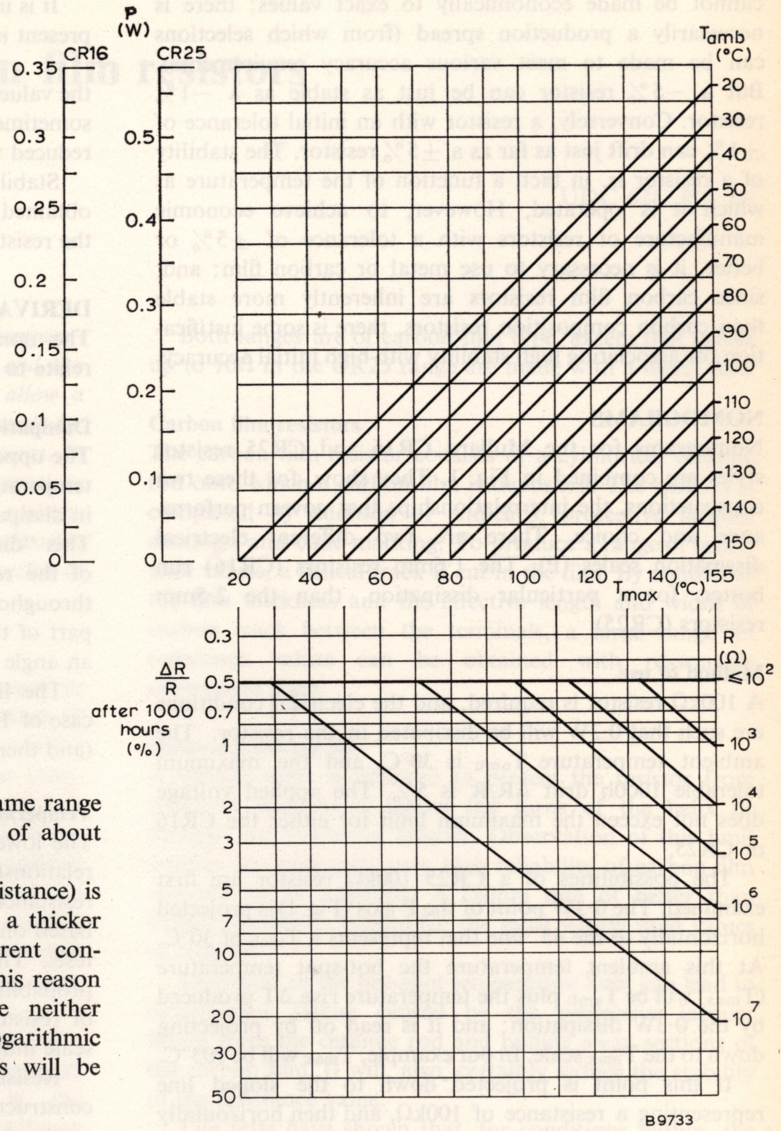

Fig. 1—Nomograms for CR16 and CR25

3%; while 1MΩ or 100kΩ resistors, from the same range and at the same temperature, will have drifts of about 0·9% and 0·5% respectively.

A thin carbon film (that is, with a higher resistance) is less stable, at any particular temperature, than a thicker carbon film. But the helical groove has different configurations for different resistance values. For this reason the lines relating to different resistances are neither parallel nor spaced in a strictly linear or logarithmic fashion. Interpolations for intermediate values will be approximate.

Other factors

The life tests on which the drift values are based were performed on complete production spreads of resistors, including (for each value and type of resistor) samples with initial values extending throughout the appropriate tolerances. A −5% resistor will, in a life test that has been set up to provide a particular dissipation in nominal resistors, in fact run at a higher dissipation; while a +5% resistor will run correspondingly cooler and will drift less. These effects have been allowed for in the nomograms.

Voltage limitations have not been taken into account in the construction of the nomograms. If resistors from, say, the CR25 range, with resistance values from a few ohms to several megohms, are life tested, the observed drift will be greater for the higher value resistors. However, above a certain value of resistance it would be necessary to apply an excessive voltage to produce the higher levels of dissipation. Limitation of the voltage to the maximum permitted value would mean that the high-value resistors would be running at a lower dissipation than low-value resistors; and they would apparently be more stable. For the present ranges of resistors, and the operating conditions covered by the nomograms, the question is academic. Attention to the voltage and current conditions that are to be met, and the use of the actual dissipation value P that the resistors will have to withstand, will provide the correct answers from the nomograms.

METAL FILM RESISTORS

Even better stabilities are attained by Mullard metal film resistors style MR25 or MR30. For example, the 1000-hour stability of an MR25 100kΩ metal film resistor at 0·3W, T_{amb} 30°C, will be about 0·11% compared with the value of 0·6% quoted on the preceding page for style CR25. A resistance drift of 0·6% would not be seen until something like 20 000 hours.

A full analysis of the capabilities of metal film resistors will be found in **Mullard Technical Communications**, Vol. 11, No. 104, March 1970, pp. 94 to 100: the article is available as a reprint, reference TP1179.

This article is a revised version of the article that appeared in **Mullard Technical Communications**, Vol. 9, No. 86, March 1967.

The basis of a design for a reversible drive with regenerative braking

J. M. LAVALLEE and J. MERRETT
Mullard Central Application Laboratory

UDC 621.316.718: 621.316.719.3: 621.313.223: 621.382.332.4

The design for a three-phase reversible d.c. motor speed-control system is described. The drive uses two fully controlled thyristor bridges connected in inverse-parallel to drive the motor, and the control system is constructed from a small number of the new Mullard power-control modules. Accurate control over a wide speed range is achieved, and the system can control motors up to at least 100hp.

INTRODUCTION

The advantages of static control equipment using thyristors for the speed control of d.c. motors are well known. Relatively simple systems may be used in a great many applications where only speed or positive-torque control is required. There are, however, a number of applications where controlled deceleration and reversing is an essential requirement. Examples of this type of application are lifts and hoists, some reeling drives, and machine tools. Regenerative braking and contactorless reversing extend the advantages of all-static drives into these more specialised fields.

This article describes a three-phase regenerative reversing speed and torque control system. The thyristor control system is constructed from a small number of universal circuit blocks. The power that can be controlled by the drive depends on the thyristor stack used, and systems of this type can be constructed to control motors up to at least 100hp.

The simplified specification of the control system is listed below.

Speed range:	500 to 1 continuously adjustable, linearity 0·2%
Torque range:	10 to 1 continuously adjustable
Speed error measured at maximum speed	±0·3% for supply variation of ±15%
	±0·1% for torque variation from 10 to 100%
	±0·2% for temperature variation from 0 to 60°C

BASIC SYSTEM DESIGN

The power control system makes use of two three-phase fully controlled bridges connected in inverse-parallel so that reversing and regenerative braking are possible under all conditions of operation. A special circuit arrangement is used to ensure that control is transferred from one bridge to the other only when the load current is zero, and then only after a short delay. The circuit is also designed to provide accurate control of the current during acceleration and changes in speed or direction. This is in addition to the normal current limit circuit which may also be used for torque control.

The block diagram of the control system is shown in Fig. 1. There are four main sections: the controlled system comprising the power controller and the mechanical units, the controller, the comparator, and the current limit. These four sections are combined to give the three feedback loops shown. Since the main function of the current limit section is to protect the final control element, it is arranged that current limit does not take effect during the normal operation of the control circuit, and so does not influence the control action.

The controlled system has an input signal v_c and an output signal v_t (the tachometer voltage proportional to motor speed). Signal v_t is fed back by loop 1 to the comparator, point 1. The difference between the reference voltage and signal v_t is the error signal which is fed to amplifier A_1 in the controller. When the amplitude of the error signal is large, the small proportional band of amplifier A_1 is exceeded and the output voltage is limited. This fixed output voltage provides one input signal V_o to the second amplifier A_2. Signal V_o is combined with signal E_m, proportional to the motor armature voltage, and the control action of loop 2 reduces the control loop error so that the error signal in loop 1 becomes small. The output voltage of amplifier A_1 is therefore reduced to below the limiting value. The high amplification of loop 1 then reduces the remaining error signal to a very small value. The control loop settles at an operating point determined by the reference voltage, at which point the effect of the positive feedback action of loop 2 is balanced by the negative feedback of loop 1.

The control principle used in this system has several advantages. When the error amplitudes are large, the very high gain of loop 1 is inoperative. The loop is in effect out of circuit, so that instability which may otherwise occur is avoided. The value of signal V_o is limited by the small pro-

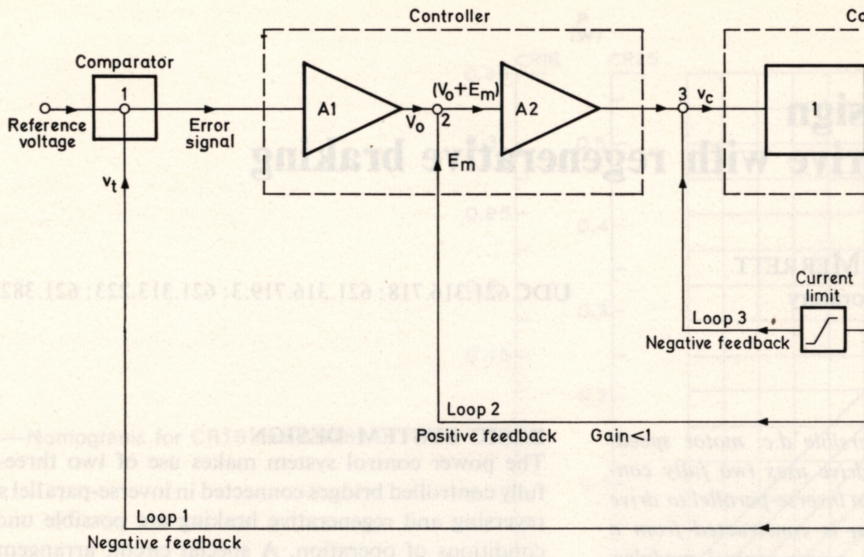
Controller
Controlled system
Comparator
1
Reference voltage
Error signal
V_t
A1
V_o
2
(V_o+E_m)
A2
3 v_c
1
2
E_m
V_t
Current limit
Loop 3
Negative feedback
Loop 2
Positive feedback
Gain<1
Loop 1
Negative feedback
9/1

Fig. 1—Simple block diagram of control system

portional band of amplifier A_1. Since amplifier A_2 and the controlled system only have proportional action, signal E_m is also limited. In the actual control system, signal E_m is derived from the armature voltage of the d.c. machine, and so current limiting in the armature circuit is obtained. This takes the form of peak current limiting.

To ensure good dynamic control characteristics, the amplification of loop 2 is made slightly less than unity. This means that in the steady state, the control voltage v_c is determined by signal E_m and not by the amplifier output V_o. The combined action of loop 1 and loop 2 results in an increase in accuracy as the speed error becomes smaller. The dynamic matching of the controller to the remainder of the system is not critical.

FUNCTIONAL SECTIONS OF THE SYSTEM

The simple block diagram of Fig. 1 has been expanded to the more detailed block diagram of Fig. 2. The actual control system, in common with most modern electronic equipment, is divided into a number of units to simplify construction and servicing. These separate units are largely functional and correspond to the blocks shown in Fig. 2. The units enclosed by the bold broken lines correspond to the main blocks of Fig. 1.

The Logic Unit contains supplementary digital circuits whose purpose is to ensure the correct driving and switching of the thyristors in the two three-phase bridges. The operation of the logic unit will be explained later.

Controlled system

The controlled system consists of two parts: the power controller comprising the trigger section and the thyristor bridges, and the mechanical unit formed by the d.c.motor, the tachometer, and the load.

To drive the motor in both directions and to provide regenerative braking, two thyristor bridges connected in inverse-parallel are necessary. The basic circuit of the two bridges and the motor is shown in Fig. 3. The two bridges operate in opposition in such a way that one operates as a rectifier while the other operates as an inverter, changing functions as the motor changes direction. The trigger angle of the two bridges must therefore be related. If the trigger angle of bridge 1 is α_1, then the trigger angle of the other bridge α_2 at the same time is (180°— α_1). The result of this mode of operation is that when the input reference voltage is reduced, the bridge operating as an inverter produces regenerative braking.

The control characteristic for the power controller is

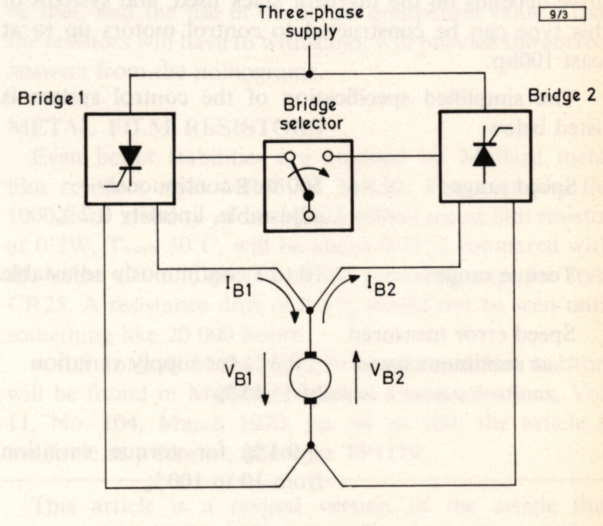
9/3
Three-phase supply
Bridge 1
Bridge selector
Bridge 2
I_{B1}
I_{B2}
V_{B1}
V_{B2}

Fig. 3—Block diagram of inverse-parallel bridges and motor

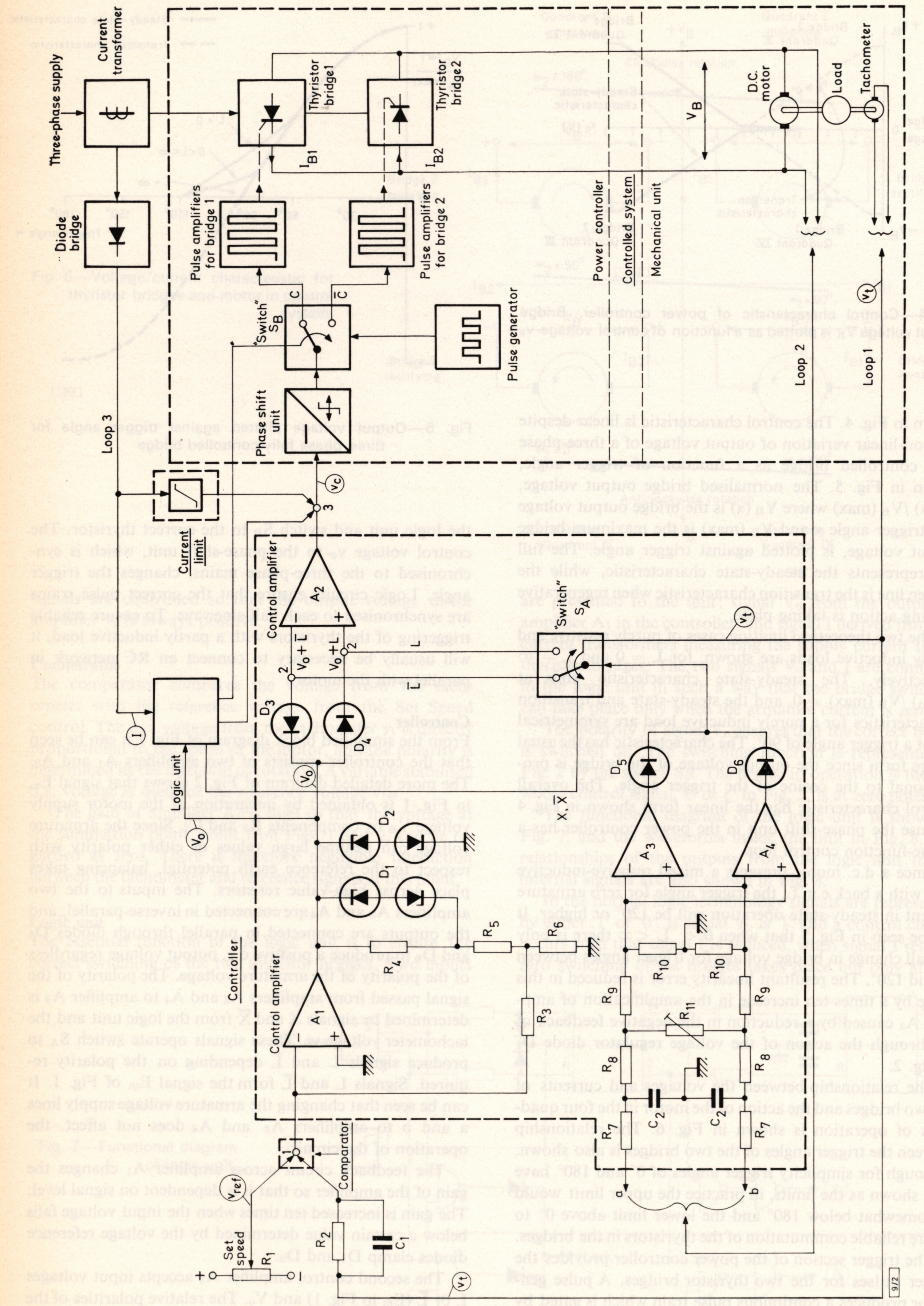
Three-phase supply
Current transformer
Diode bridge
Thyristor bridge1
Thyristor bridge2
I_{B1}
I_{B2}
Pulse amplifiers for bridge 1
Pulse amplifiers for bridge 2
C
$\bar{C}$
"Switch" S_B
Pulse generator
Phase shift unit
Loop 3
Current limit
v_c
3
Power controller
Controlled system
Mechanical unit
V_B
D.C. motor
Load
Tachometer
Loop 2
Loop 1
V_t
Control amplifier
A_2
$V_o+\Gamma$
V_o+L
2
L
Γ
"Switch" S_A
X, X
Logic unit
D_3
D_4
D_1
D_2
D_5
D_6
V_o
A_3
A_4
R_4
R_5
R_6
R_{10}
R_9
R_{11}
R_8
R_7
C_2
a
b
Controller
Control amplifier
A_1
R_3
Comparator
V_{ref}
Set speed
R_1
R_2
C_1
1
9/2

Fig. 2—More detailed diagram of control system showing functional elements

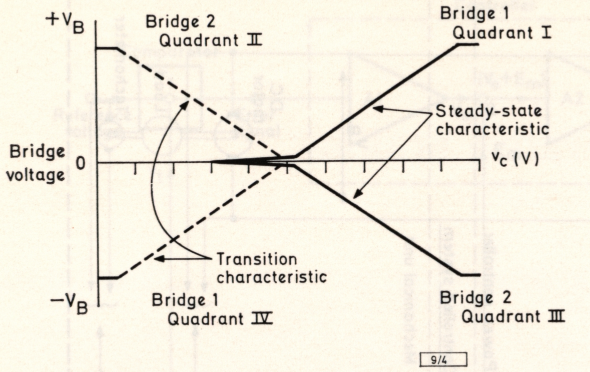

Fig. 4—Control characteristic of power controller. Bridge output voltage V_B is plotted as a function of control voltage v_c

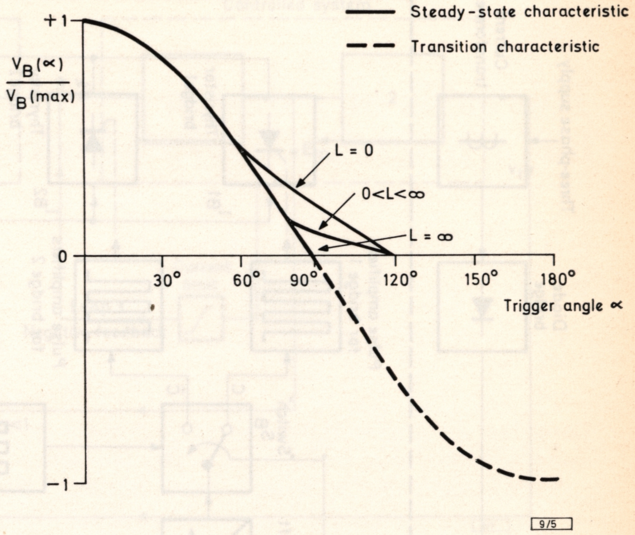

Fig. 5—Output voltage plotted against trigger angle for three-phase fully controlled bridge

shown in Fig. 4. The control characteristic is linear despite the non-linear variation of output voltage of a three-phase fully controlled bridge as a function of trigger angle, shown in Fig. 5. The normalised bridge output voltage, $V_B (\alpha) / V_B$ (max) where $V_B (\alpha)$ is the bridge output voltage at a trigger angle α and V_B (max) is the maximum bridge output voltage, is plotted against trigger angle. The full line represents the steady-state characteristic, while the broken line is the transition characteristic when regenerative braking action is taking place.

The two theoretical limiting cases of purely resistive and purely inductive loads are shown, for $L = 0$ and $L = \infty$ respectively. The steady-state characteristic ends at $V_B (\alpha) / V_B (\text{max}) = 0$, and the steady-state and transition characteristics for a purely inductive load are symmetrical about a trigger angle of 90°. The characteristic has the usual cosine form since the output voltage of the bridge is proportional to the cosine of the trigger angle. The overall control characteristic has the linear form shown in Fig. 4 because the phase-shift unit in the power controller has a cosine-function control loop.

Since a d.c. motor presents a mixed resistive-inductive load with a back e.m.f., the trigger angle for zero armature current in steady-state operation will be 120° or higher. It can be seen in Fig. 5 that when $0 < L < \infty$ there is only a small change in bridge voltage for trigger angles between 90 and 120°. The resultant linearity error is reduced in this range by a times-ten increase in the amplification of amplifier A_1 caused by a reduction in the negative feedback of A_1 through the action of the voltage regulator diode D_1 in Fig. 2.

The relationship between the voltages and currents of the two bridges and the action of the motor in the four quadrants of operation is shown in Fig. 6. The relationship between the trigger angles of the two bridges is also shown. Although for simplicity trigger angles of 0° and 180° have been shown as the limits, in practice the upper limit would be somewhat below 180° and the lower limit above 0° to ensure reliable commutation of the thyristors in the bridges.

The trigger section of the power controller provides the trigger pulses for the two thyristor bridges. A pulse generator produces a continuous pulse train which is gated by the logic unit and switch S_B to the correct thyristor. The control voltage v_c to the phase-shift unit, which is synchronised to the three-phase mains, changes the trigger angle. Logic circuits ensure that the correct pulse trains are synchronised to each half-sinewave. To ensure reliable triggering of the thyristors with a partly inductive load, it will usually be necessary to connect an RC network in parallel with the motor.

Controller

From the simplified block diagram of Fig. 1 it can be seen that the controller consists of two amplifiers A_1 and A_2. The more detailed diagram of Fig. 2 shows that signal E_m in Fig. 1 is obtained by integration of the motor supply voltage V_B by components R_7 and C_2. Since the armature voltage can assume large values of either polarity with respect to the reference earth potential, balancing takes place across high-value resistors. The inputs to the two amplifiers A_3 and A_4 are connected in inverse-parallel, and the outputs are connected in parallel through diodes D_5 and D_6 to produce a positive d.c. output voltage regardless of the polarity of the armature voltage. The polarity of the signal passed from amplifiers A_3 and A_4 to amplifier A_2 is determined by signals X and $\overline{X}$ from the logic unit and the tachometer voltage v_t. These signals operate switch S_A to produce signals L and $\overline{L}$ depending on the polarity required. Signals L and $\overline{L}$ form the signal E_m of Fig. 1. It can be seen that changing the armature voltage supply lines a and b to amplifiers A_3 and A_4 does not affect the operation of the circuit.

The feedback circuit across amplifier A_1 changes the gain of the amplifier so that it is dependent on signal level. The gain is increased ten times when the input voltage falls below a certain value determined by the voltage reference diodes clamp D_1 and D_2.

The second control amplifier A_2 accepts input voltages L or $\overline{L}$ (E_m in Fig. 1) and V_o. The relative polarities of the signals are controlled so that the output voltage of the amplifier v_c is always positive.

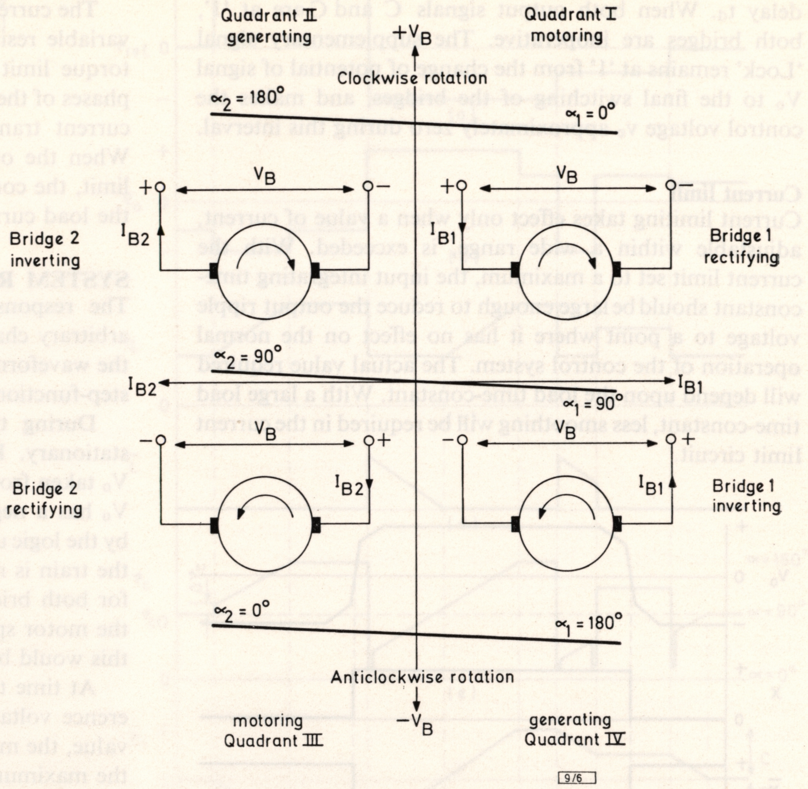

Fig. 6—Voltage/current characteristic for thyristor bridges and motor in control system.

Comparator

The comparator compares the voltage from the tachometer with the reference voltage from the Set Speed control. The d.c. voltage from the tachometer v_t is directly proportional to the speed of the motor, and the polarity is determined by the direction of rotation. A variable stabilised d.c. voltage is used for the reference voltage v_{ref}.

The gain of amplifier A_1 is high so that the voltage at the summation point, point 1 on Figs. 1 and 2, can be regarded as zero. There is therefore negligible interaction between the tachometer and reference signals at this point.

Logic unit

The essential function of the logic unit is to ensure the correct switching of the two thyristor bridges. Two inputs are presented to the unit: signal V_o from the output of amplifier A_1 in the controller, and signal I derived from the current transformers measuring the supply current to the thyristor bridges. The two signals V_o and I are combined in the logic unit in such a way that the bridge switching can take place only when the armature current is zero.

The polarity of signal V_o ensures that the correct bridge is switched on. The switching function is represented in Fig. 2 by the switch S_B. The bridge in operation is the one whose control signal, C or C in Fig. 2, is at zero potential.

The functional diagram of the logic unit is shown in Fig. 7, and the waveforms inside the unit in Fig. 8. The relationships of the outputs from the logic unit to the internal signals are also shown in Fig. 8.

In the normal logic terminology signals are represented by either ‘1’ or ‘0’. If signal V_o is ‘1’ and a control change occurs such that signal I is reduced, when signal I reaches zero switching of the bridges takes place but only after a

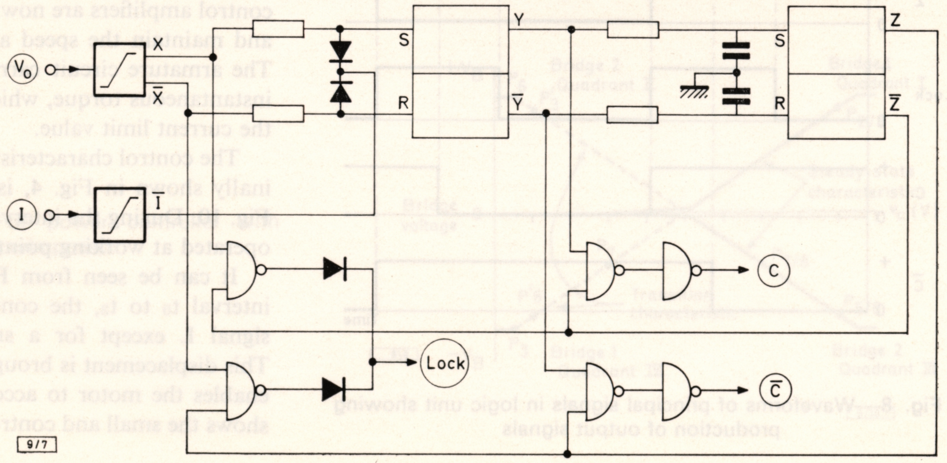

Fig. 7—Functional diagram of logic unit.

delay t_d. When both output signals C and $\overline{C}$ are at '1', both bridges are inoperative. The supplementary signal 'Lock' remains at '1' from the change of potential of signal V_o to the final switching of the bridges, and makes the control voltage v_c approximately zero during this interval.

Current limit

Current limiting takes effect only when a value of current, adjustable within a wide range, is exceeded. With the current limit set to a maximum, the input integrating time-constant should be large enough to reduce the output ripple voltage to a point where it has no effect on the normal operation of the control system. The actual value required will depend upon the load time-constant. With a large load time-constant, less smoothing will be required in the current limit circuit.

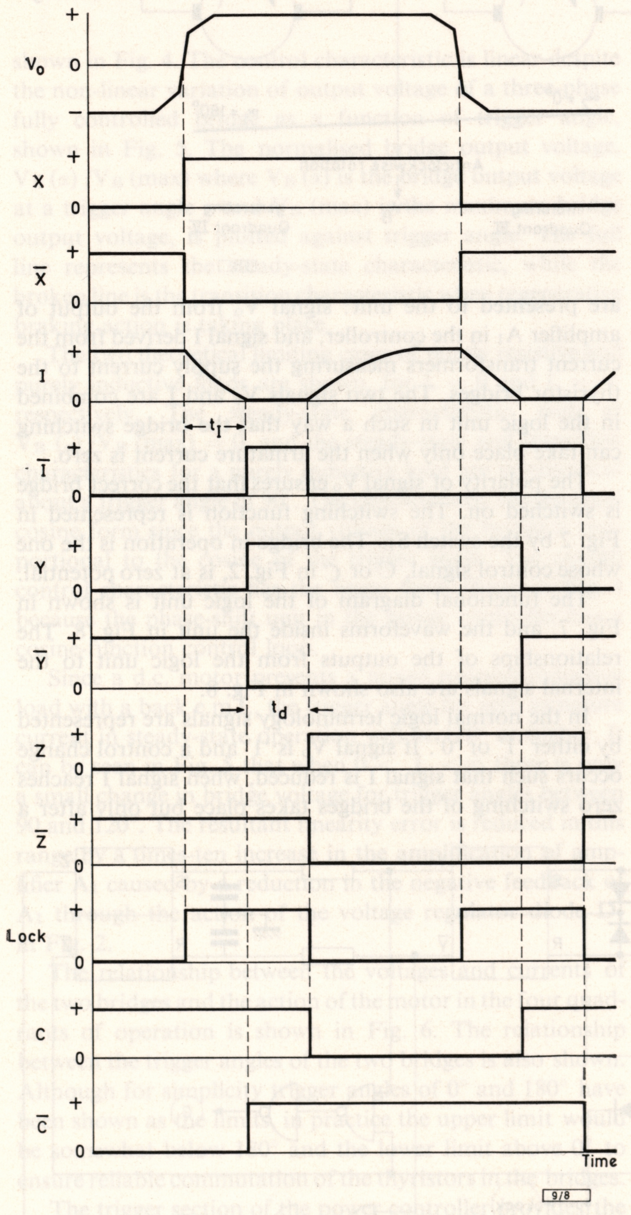
V_o
X
$\overline{X}$
I
$\overline{I}$
Y
$\overline{Y}$
Z
$\overline{Z}$
Lock
C
$\overline{C}$
+
0
−
t_1
t_d
Time
9/8

Fig. 8—Waveforms of principal signals in logic unit showing production of output signals

The current limit value is made variable, by means of a variable resistor, so that it can be used as an adjustable torque limit control. The current is sensed in the three phases of the mains supply to the thyristor bridges by three current transformers which feed three bridge rectifiers. When the output voltage of the bridge exceeds a preset limit, the control voltage v_c is affected in such a way that the load current is kept constant.

SYSTEM RESPONSE TO STEP INPUT

The response of the complete control system to an arbitrary change in the reference voltage v_{ref} is shown by the waveforms in Fig. 9. The waveforms give the idealised step-function response for continuous armature current.

During the interval t_0 to t_1, $v_{ref} = 0$ and the motor is stationary. Because of the high gain of amplifier A_1, signal V_o taken from the output is not exactly zero. When signal V_o has a negative value, the trigger pulse train is routed by the logic unit to thyristor bridge 1. With a positive value, the train is routed to bridge 2. It is therefore not possible for both bridges to receive pulses simultaneously, even if the motor speed is zero, although in a theoretical system this would be the case.

At time t_1 there is a positive abrupt change of the reference voltage. If the change is to the maximum positive value, the motor must change to a speed corresponding to the maximum armature voltage. The waveforms of Fig. 9 show how this takes place.

The change in reference voltage v_{ref} is shown in Fig. 9a. Even in response to a positive change in the reference voltage of only a few millivolts, signal V_o almost reaches its limit value, as shown in Fig. 9b. This produces a small change in the control voltage, Δv_c in Fig. 9e, which produces in turn a change in bridge voltage ΔV_B, as shown in Fig. 9k. Thus the maximum possible step increase in armature current is limited to $\Delta V_B/R_A$, where R_A is the armature resistance. The further increase in signal V_o of one or two millivolts resulting from the full change in v_{ref} has a negligible effect on the control system at time t_1. The armature current increases to the value designated the maximum possible limit value in Fig. 9g. The current limit, operating after a delay, reduces the armature current to a preselected value (designated the current limit level in Fig. 9g). The motor accelerates with constant current to the maximum forward speed.

At a time t_2, the motor reaches its nominal speed. Both control amplifiers are now in their linear amplifying range, and maintain the speed accurately to a controlled value. The armature circuit carries the current required by the instantaneous torque, which in all cases must be less than the current limit value.

The control characteristic of the power controller, originally shown in Fig. 4, is shown again in more detail in Fig. 10. During the interval t_2 to t_3, the thyristor bridge is operated at working point $P_{2/3}$.

It can be seen from Figs. 9c and 9e that during the interval t_0 to t_3, the control voltage v_c is controlled by signal L except for a small vertical displacement Δv_c. This displacement is brought about by control loop 1, and enables the motor to accelerate with constant current. It shows the small and controlled effect of an abrupt change

Fig. 9—Response of control system to change of input signal

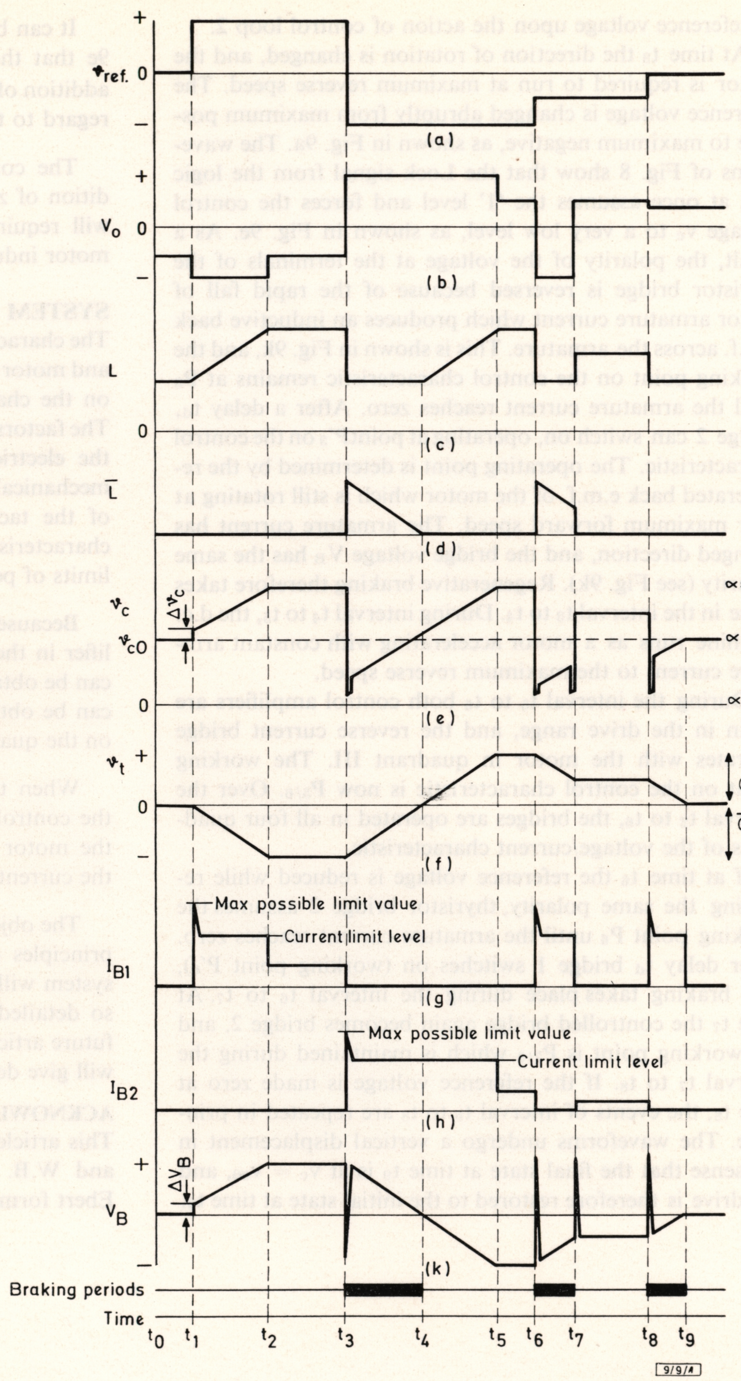
$v_{ref.}$
V_o
L
$\overline{L}$
v_c
v_{cO}
Δv_c
v_t
I_{B1}
I_{B2}
V_B
ΔV_B
+
0
−
(a)
(b)
(c)
(d)
(e)
(f)
(g)
(h)
(k)
∝=180°
∝=90°
∝=0°
C
$\overline{C}$
Max possible limit value
Current limit level
Max possible limit value
Current limit level
Braking periods
Time
t_0
t_1
t_2
t_3
t_4
t_5
t_6
t_7
t_8
t_9
9/9/A

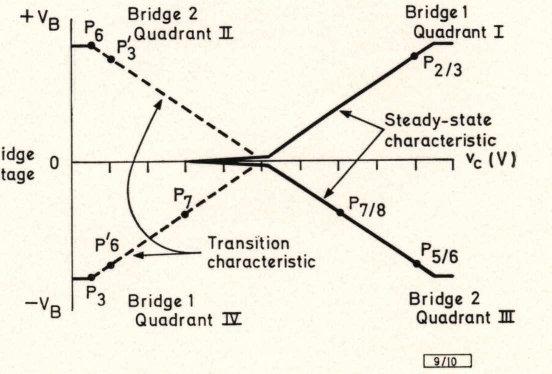
$+V_B$
$-V_B$
Bridge voltage
0
v_c (V)
Bridge 2 Quadrant II
Bridge 1 Quadrant I
Bridge 1 Quadrant IV
Bridge 2 Quadrant III
P_6
P'_3
$P_{2/3}$
Steady-state characteristic
P_7
$P_{7/8}$
P'_6
Transition characteristic
P_3
$P_{5/6}$
9/10

Fig. 10—Control characteristic of power controller with working points superimposed

of reference voltage upon the action of control loop 2.

At time t_3 the direction of rotation is changed, and the motor is required to run at maximum reverse speed. The reference voltage is changed abruptly from maximum positive to maximum negative, as shown in Fig. 9a. The waveforms of Fig. 8 show that the Lock signal from the logic unit at once assumes the '1' level and forces the control voltage v_c to a very low level, as shown in Fig. 9e. As a result, the polarity of the voltage at the terminals of the thyristor bridge is reversed because of the rapid fall of motor armature current which produces an inductive back e.m.f. across the armature. This is shown in Fig. 9k, and the working point on the control characteristic remains at P_3 until the armature current reaches zero. After a delay t_d, bridge 2 can switch on, operating at point P'_3 on the control characteristic. The operating point is determined by the regenerated back e.m.f. of the motor which is still rotating at near maximum forward speed. The armature current has changed direction, and the bridge voltage V_B has the same polarity (see Fig. 9k). Regenerative braking therefore takes place in the interval t_3 to t_4. During interval t_4 to t_5, the d.c. machine runs as a motor accelerating with constant armature current to the maximum reverse speed.

During the interval t_5 to t_6 both control amplifiers are again in the drive range, and the reverse current bridge operates with the motor in quadrant III. The working point on the control characteristic is now $P_{5/6}$. Over the interval t_2 to t_6, the bridges are operated in all four quadrants of the voltage/current characteristic.

If at time t_6 the reference voltage is reduced while retaining the same polarity, thyristor bridge 2 assumes the working point P_6 until the armature current reaches zero. After delay t_d bridge 1 switches on (working point P'_6), and braking takes place during the interval t_6 to t_7. At time t_7 the controlled bridge again becomes bridge 2, and the working point is $P_{7/8}$ which is maintained during the interval t_7 to t_8. If the reference voltage is made zero at time t_8, the events of interval t_6 to t_8 are repeated in principle. The waveforms undergo a vertical displacement in the sense that the final state at time t_9 is at $v_c = v_{c0}$, and the drive is therefore restored to the initial state at time t_0.

It can be seen from the waveforms of Figs. 9c, 9d, and 9e that the control voltage v_c results in effect from the addition of signals L and $\bar{L}$ in the correct polarity, with due regard to the effect of the Lock signal.

The control voltage v_{c0} represents the dynamic condition of zero motor speed. In practice, static zero speed will require a slightly different value of v_c because the motor inductance has a finite value (as shown in Fig. 5).

SYSTEM CHARACTERISTICS

The characteristics of the overall system (the control system and motor and load being driven) will depend to some extent on the characteristics of the motor and load themselves. The factors that can affect the overall characteristics include the electrical time-constant of the motor armature, the mechanical time-constant of the motor, and the quality of the tachometer used. These factors rather than the characteristics of the control system may well define the limits of performance of the overall system.

Because of the high proportional gain of the first amplifier in the controller, the accuracy of speed control that can be obtained can be better than 1%. The accuracy that can be obtained in practice, however, depends very much on the quality of the tachometer and the reference voltage.

When the control system is in continuous operation, the control rate is governed by the moment of inertia of the motor and load, the load circuit time-constant, and the current loading capacity of the motor.

The object of this article has been to describe the design principles of the control system. The performance of a system will depend on the details of the circuit used, and so detailed performance figures cannot be given here. A future article will deal in detail with the circuit design, and will give detailed performance figures.

ACKNOWLEDGEMENTS

This article incorporates information from E.B.G. Nijhof and W.B. Rosink of C.A.B. Elcoma, Eindhoven, and Ebert formerly of Valvo GmbH, Hamburg.